Primary particle size effect on phase transition in $Ba_2In_2O_5$

J.F.Q. Rey [a,b], F.F. Ferreira [b], E.N.S. Muccillo [a,*]

[a] Energy and Nuclear Research Institute-IPEN, PO BOX 11049, S. Paulo, SP, 05422-970, Brazil
[b] Brazilian Synchrotron Light Laboratory-LNLS, PO BOX 6192, Campinas, SP, 13083-970, Brazil

Abstract

The primary particle (or crystallite) size effect on the order–disorder phase transition temperature in $Ba_2In_2O_5$ was investigated. Sintered specimens were prepared by solid state synthesis. Structural characterization performed by Raman spectroscopy shows that single-phase brownmillerite structure was obtained at room temperature for all prepared samples. *In situ* high-temperature X-ray diffraction experiments using Synchrotron radiation and electrical conductivity measurements reveal a decrease in the phase transition temperature with decreasing of the primary particle size. Lattice defects, mainly hydroxyls and nitrates, also influence the phase transition in $Ba_2In_2O_5$.
© 2007 Elsevier B.V. All rights reserved.

1. Introduction

Oxygen-ion conductors have been extensively studied as a consequence of their potential technological applications, such as oxygen sensors and monitors, electrolytes in solid oxide fuel cells, and oxygen permeable membranes [1].

Oxide ceramics with cubic perovskite or related structures may exhibit high oxygen-ion conductivity [1]. The mixed oxide $Ba_2In_2O_5$ adopts an orthorhombic structure from room temperature up to 925 °C with cell parameters $a=0.608$ nm, $b=1.679$ nm and $c=0.589$ nm [2]. At that temperature, an order–disorder phase transition occurs and the crystalline structure changes to tetragonal symmetry. A second-order phase transition at 1040 °C turns the crystalline structure to cubic perovskite, when the anionic vacancies are in a fully disordered state [3,4], and the mixed oxide exhibits pure ionic conduction with unity ionic transport number [5,6].

Great attention has been given over the last few years to the effects imparted by the physical properties of particles, like size, shape and size distribution, on bulk ceramics and thin films properties. Recent reports on bulk ceramics have shown a size-dependent tetragonal stability in $PbTiO_3$ [7] and $BaTiO_3$ [8] nanocrystals. In multiferroic $BiFeO_3$ a particle size dependent magnetization and phase transition was noticed [9]. Complete maghemite to haematite phase transition was achieved at relatively lower temperatures with decreasing of the particle size [10]. In addition, changes in the α-β phase transition temperature in $La_2Mo_2O_9$ ionic conductor was also observed as a particle size effect [11].

In this work the primary particle size effect on the order–disorder phase transition temperature of $Ba_2In_2O_5$ was investigated by *in situ* high-temperature X-ray diffraction and electrical conductivity measurements.

2. Experimental

$BaCO_3$ (99.8%, Alfa Aesar), In_2O_3 (99.99%, Aldrich) and In $(NO_3)_3 \cdot H_2O$ (99.99%, Alfa Aesar) were used as starting materials. $Ba_2In_2O_5$ powders with different particle sizes were prepared by the conventional solid state synthesis process using mixtures of oxide and carbonate precursors (samples type S1 and S2) or nitrate precursors (samples designated as N). To obtain a lower particle size, the starting oxide and carbonate

---
* Corresponding author. Energy and Nuclear Research Institute-CCTM, PO BOX 11049, S. Paulo, SP, 05422-970, Brazil. Tel.: +55 11 38169343; fax: +55 11 38169370.
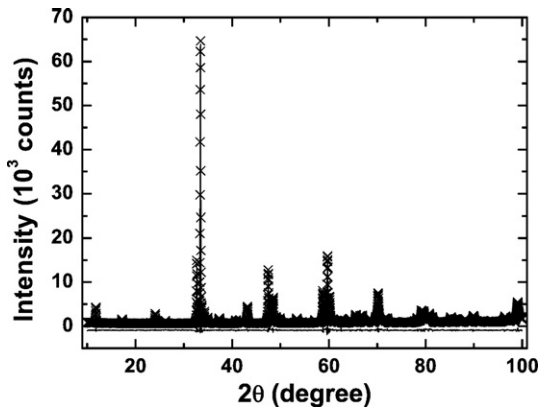*E-mail address:* enavarro@usp.br (E.N.S. Muccillo).

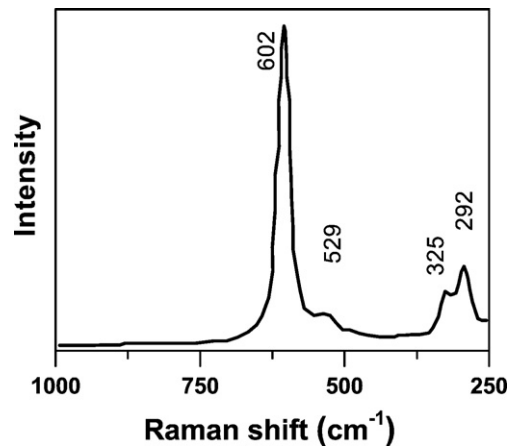Fig. 1. Room temperature X-ray diffraction pattern of sample type N.

Fig. 2. Room temperature Raman spectrum of sample type S1.

precursors were milled together (S2-type samples). Cylindrical pellets were prepared by pressing and sintering at 1300 °C or 1350 °C.

Structural characterization was done by X-ray diffraction (XRD) using a conventional diffractometer (D8 Advance, Bruker-AXS) and the XPD D10B beam line of the Brazilian Synchrotron Light Laboratory (LNLS). The crystal structures of $Ba_2In_2O_5$ were determined through Rietveld refinement using GSAS. The primary particle sizes were determined from broadened diffraction lines directly from refined patterns [12]. The apparent domain size determined is averaged for all domains within the diffracting volume, in this case. Raman spectroscopy (Renishaw Raman microscope system 3000) was also used for phase characterization. Phase transition study was carried out by *in situ* high-temperature X-ray diffraction (at LNLS) and electrical conductivity by impedance spectroscopy measurements (HP 4192A LF impedance analyzer).

3. Results and discussion

3.1. Structural characterization

Room temperature X-ray diffraction results show that all prepared materials were well crystallized brownmillerite-type structure with orthorhombic symmetry. Fig. 1 shows, as an example, the diffraction pattern of sample N. In this case, the XRD pattern was obtained in the XPD D10B beam line of LNLS.

The room temperature lattice parameters, the primary particle (or crystallite) size and cell volume determined from Rietveld refinement are summarized in Table 1.

Crystallographic data of samples S1 and N are similar to each other and to those of previous works [2,13]. The particle size of all samples is within the nanosize range, although they greatly differ.

Fig. 2 shows the Raman spectrum of sample S1. The brownmillerite-type structure of $Ba_2In_2O_5$ is known to exhibit several active Raman modes in the 80 to 605 cm^{-1} spectral range. The most intense Raman band has its maximum amplitude at 602 cm^{-1} followed by 292 cm^{-1} and 325 cm^{-1}, respectively [14]. No Raman band that could be attributed to other phase in the $BaO–In_2O_3$ system is observed in this spectrum. Similar results were obtained for all the studied samples. This result ensures that single phase $Ba_2In_2O_5$ samples were obtained independent on the processing parameters used to prepare the sintered materials.

3.2. Phase transition

A special setup [15] was used for *in situ* high-temperature X-ray diffraction study of the order–disorder phase transition in $Ba_2In_2O_5$. Fig. 3 shows XRD patterns detected in the room temperature to 950 °C temperature range. It is evident that at

Table 1
Room temperature lattice constants (a, b and c), particle size (D), and cell volume (V) of sintered specimens

	a (nm)	b (nm)	c (nm)	D (nm)	V (nm^3)
S1[a]	0.60912	1.6738	0.59623	110.7	0.6079
S2[a]	0.60414	1.68863	0.59746	32	0.6095
N[b]	0.60968	1.67209	0.59626	142.1	0.6078

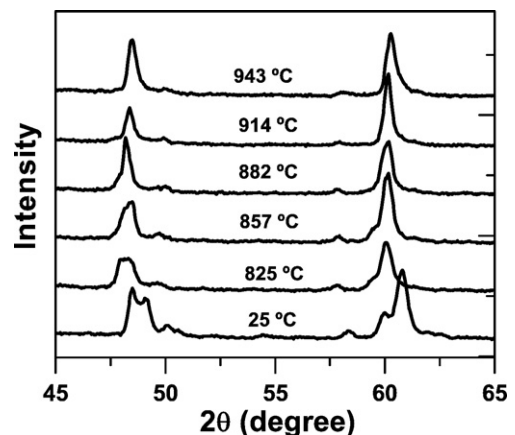Data obtained using a [a]diffractometer and [b]Synchrotron radiation.

Fig. 3. *In situ* high-temperature X-ray diffraction patterns of sample type N.
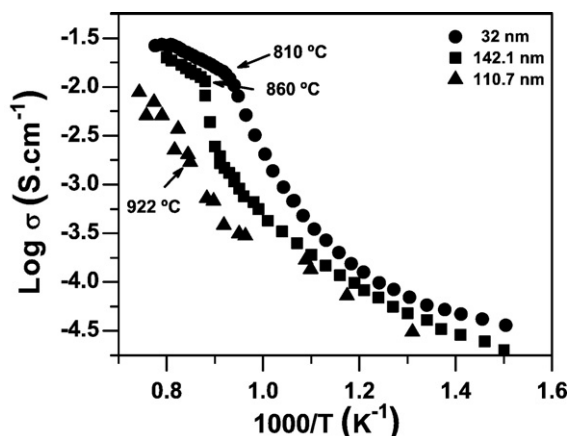
Fig. 4. Arrhenius plots of the electrical conductivity of $Ba_2In_2O_5$ sintered materials.

825 °C the phase transition has already started. This temperature is relatively lower than that reported in the literature.

Fig. 4 shows Arrhenius plots of the electrical conductivity of $Ba_2In_2O_5$ sintered materials. There is a continuous increase in the electrical conductivity with increasing temperature, and suddenly a sharp increase in the magnitude of the conductivity reveals the first order phase transition. It is important to note that the onset of the order–disorder phase transition vary with the particle size. Specimens type S1 have an onset temperature of about 922 °C in agreement with reported values [2,4], whereas for S2 samples that temperature is only 810 °C.

The difference in the phase transition temperature of S-type samples deserves attention. The main difference in these samples is the room temperature particle size. In addition, this variable influences the cell parameters and the cell volume. It is generally known that the lower is the particle size the higher is the surface energy of a system. Moreover, surface energy is known to have an effect on crystal lattice distortion, which in turn affects the phase transition temperature. Thus, it seems that the particle size is the dominating factor affecting the phase transition temperature in $Ba_2In_2O_5$ mixed oxide. A full account of the primary particle size effect on electrical conductivity of $Ba_2In_2O_5$ will be the subject of a forthcoming publication.

The cell parameters and cell volumes of samples S1 and N are similar, although the particle size of the latter is higher, but the phase transition temperature is still lower. Now, the discussion is mainly on the influence of lattice defects that might be inserted in $Ba_2In_2O_5$ during synthesis. Results of infrared spectroscopy, not presented here, show that sintered N samples contain adsorbed OH^- and NO_3^- species. Entrapment of OH species might occur at an oxygen vacancy site, and thus, a decrease in the available vacancy sites for conduction is

expected. Then, hydroxyl entrapment in the crystal lattice is an adverse effect that may reduce the ionic conductivity of the sintered material. Thermogravimetric measurements under isothermal conditions at 1350 °C on sintered materials show that a weight loss (<2%) occurs. In the literature there have been several reports showing that lattice hydroxyls cause instability of the crystalline structure in $BaTiO_3$ [8], and imparts a critical size for the onset of the α-γ phase transition in Fe_2O_3 [10]. Thus, adsorbed and/or inserted species are responsible for the phase transition dependence on the particle environment. In this case hydroxyls and nitrates, seem to control the order–disorder transition temperature in $Ba_2In_2O_5$.

4. Conclusions

The phase transition temperature decreases with decreasing of the particle size. Adsorbed hydroxyls and nitrates seem to exert an additional effect on the phase transition temperature in $Ba_2In_2O_5$ mixed oxide.

Acknowledgements

References

[1] J.B. Goodenough, Ann. Rev. Mater. Res. 33 (2003) 91.
[2] J.B. Goodenough, J.E. Ruiz-Diaz, Y.S. Zhen, Solid State Ionics 44 (1990) 21.
[3] T.R.S. Prasanna, A. Navrotsky, J. Mater. Res. 8 (1993) 1484.
[4] S.B. Adler, J.A. Reimer, J. Baltisberg, U. Werner, J. Am. Chem. Soc. 116 (1994) 675.
[5] G.B. Zhang, D.M. Smith, Solid State Ionics 82 (1995) 161.
[6] T. Hashimoto, Y. Ueda, M. Yoshinaga, K. Komazaki, K. Asaoka, S. Wang, J. Electrochem. Soc. 149 (2002) 1381.
[7] E.K. Akdogan, A. Safari, J. Appl. Phys. 101 (2007) 064114.
[8] W. Sun, J. Appl. Phys. 100 (2006) 083503.
[9] R. Mazumder, S. Ghosh, P. Mondal, D. Bhattacharya, S. Dasgupta, N. Das, A. Sen, A.K. Tyagi, M. Sivakumar, T. Takami, H. Ikuta, J. Appl. Phys. 100 (2006) 033908.
[10] G. Gnanaprakash, S. Ayyappan, T. Jayakumar, J. Philip, B. Raj, Nanotechnol. 17 (2006) 5851.
[11] R.A. Rocha, E.N.S. Muccillo, J. Alloys Compd. 443 (2007) 154.
[12] R.A. Young, The Rietveld Method, Oxford Univ. Press, New York, 1993, p. 135.
[13] C.A.J. Fisher, M.S. Islam, R.J. Brook, J. Solid State Chem. 128 (1997) 137.
[14] T.A. Kalinina, L.N. Lykova, L.M. Kovba, M.G. Mel´nikova, N.V. Porotnikov, Russ. J. Inorg. Chem. 28 (1983) 259.
[15] F.F. Ferreira, E. Granado, W. Carvalho Jr., S.K. Kycia, D. Bruno, R. Droppa Jr., J. Synchrotron Radiat. 13 (2006) 46.